ADVANCED ENERGY MATERIALS
www.advenergymat.de

3D Si/C Fiber Paper Electrodes Fabricated using a Combined Electrospray/Electrospinning Technique for Li-Ion Batteries

*Yunhua Xu, Yujie Zhu, Fudong Han, Chao Luo, and Chunsheng Wang**

Although the theoretical capacity of silicon is ten times higher than that of graphite, the overall electrode capacity of Si anodes is still low due to the low Si loading and heavy metal current collector. Here, a novel flexible 3D Si/C fiber paper electrode synthesized by simultaneously electrospraying nano-Si-PAN (polyacrylonitrile) clusters and electrospinning PAN fibers followed by carbonization is reported. The combined technology allows uniform incorporation of Si nanoparticles into a carbon textile matrix to form a nano-Si/carbon composite fiber paper. The flexible 3D Si/C fiber paper electrode demonstrate a very high overall capacity of ≈1600 mAh g^{-1} with capacity loss less than 0.079% per cycle for 600 cycles and excellent rate capability. The exceptional performance is attributed to the unique architecture of the flexible 3D Si/C fiber paper, i.e., the resilient and conductive carbon fiber network matrix, carbon-coated Si nanoparticle clusters, strong adhesion between carbon fibers and Si nanoparticle clusters, and uniform distribution of Si/C clusters in the carbon fiber frame. The scalable and facile synthesis method, good mechanical properties, and excellent electrochemical performance at a high Si loading make the flexible 3D Si/C fiber paper batteries extremely attractive for plug-in electric vehicles, flexible electronics, space exploration, and military applications.

1. Introduction

Lithium ion batteries have been the most important energy storage technology for portable electronics and are critical to the emerging plug-in electric vehicles, flexible electronics, and aerospace applications. To satisfy the high energy requirements of flexible electronics, the Li-ion batteries should have high overall energy and power density, long cycling life, good flexibility, and low cost. The current graphite/$LiCoO_2$ batteries have low energy density and poor flexibility. For example, commercial graphite anodes prepared by slurry-coating on Cu current collectors show an overall capacity of only ≈200 mAh g^{-1} based on the total mass of the whole electrode in traditional battery techniques. This is due to the heavy weight of the metal current collectors and the use of binders.[1,2] To improve the overall specific capacity of an electrode, high capacity active materials and light-weight current collectors should be used.

With ten times higher theoretical capacity, abundance, non-toxicity, and low cost, Si has attracted extensive attention as an anode to replace graphite.[3–25] However, Li insertion/extraction in Si particles induces a huge volume change, leading to severe pulverization and electric disconnection of Si particles, thus reducing the cycling stability.[3] Furthermore the poor electronic conductivity of Si also lowers the power density of Si anodes. Significant improvements in the electrochemical performance of Si anodes have been achieved by using nanotechnology, including nanoparticles,[6–9] nanowires,[10,11] nanotubes,[12,13] nanofibers,[14,15] nanoporous structures,[16–18] hollow structures,[19,20] and carbon-incorporated composites.[21–25]

Currently, the Si electrodes are prepared by casting slurries that consist of Si particles, binders, and conductive additives onto Cu metal current collectors. Si loading is normally less than 1.0 mg cm^{-2}, which only accounts for a very small fraction (normally 3–5 wt%) of the total mass of the whole electrodes.[2] The capacities for Si anodes are usually calculated based on the Si mass rather than the overall mass of the entire Si anode. Although a high capacity (>2000 mAh g^{-1}) was reported in terms of mass of Si for structure-designed Si materials, the overall capacity of the entire anodes is less than 100 mAh g^{-1} if one considers the weight of the Cu current collectors. Although the increase in Si loading can enhance the overall capacity of the entire Si electrode, it will also increase the thickness of the Si electrodes on the Cu current collectors, thus lowering its robustness towards mechanical damage due to the volume change and resulting in poor cycle life.

Extensive efforts on Si/C composite design have been made. However little attention was paid to the design of electrode architectures to enhance the overall capacity and flexibility. Metal current collectors, the heaviest component in anodes, significantly reduce the overall capacity. In contrast to Cu metal, carbon materials such as carbon fibers, graphene and carbon

Dr. Y. Xu, Dr. Y. Zhu, F. Han, C. Luo, Prof. C. Wang
Department of Chemical and Biomolecular Engineering
University of Maryland
College Park, MD 20742, USA
E-mail: cswang@umd.edu

DOI: 10.1002/aenm.201400753

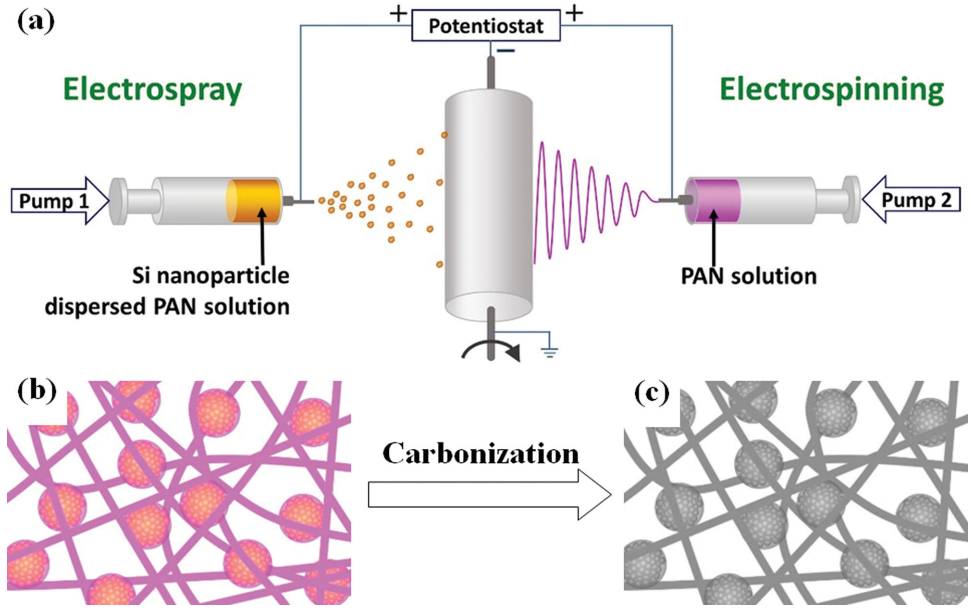

Figure 1. Schematic illustration of a) the synthesis process and the architecture of the flexible 3D Si/C fiber paper electrode b) before and c) after carbonization.

nanotubes, offer light weight, excellent electric conductivity, and good mechanical properties, making them very attractive as alternative current collectors.[1,2,26–34] Carbon paper with a mass several times lower than Cu foil has been successfully used as a current collector, improving the relative mass loading of Si. Guo et al. reported a high overall capacity of 728 mAh g^{-1} of Si-C anodes with carbon paper current collectors, which is four times higher than that of graphite anodes.[26] However, it is challenging to load a larger quantity of Si nanoparticles onto carbon paper using the traditional slurry-casting technique. Lee et al. developed a graphene-supported self-standing Si/graphene film anode by filtering a mixture dispersion of Si nanoparticles and graphene sheets.[27] High capacity was demonstrated, but the low diffusion rate of Li ions through the Si/graphene films limited the rate capability. Chemical vapor deposition (CVD) of Si nanoparticles on a CNT matrix has been investigated by several groups. However, the poor cycling stability due to the inherently weak adhesion between the Si and CNTs limits the cycling stability.[1,30,31] Additionally, the synthesis of graphene and CNTs requires precise control, making them unsuitable for practical mass production. To date, flexible Si anodes with high capacity, good rate capability, and long cycle life have not been achieved.

Electrospinning and electrospray have been used as techniques to produce composite nanofibers and nanoparticles for Li-ion batteries.[14,15,20,37–45] Both electrospinning and electrospray use high electric fields to produce a liquid jet. In electrospray, liquid droplets are formed due to the higher electric force compared to the surface tension of the low solution viscosity; in electrospinning, fibers are extruded from a polymer solution that can produce a continuous jet stretch with an electric repulsion force. Electrospinning can produce various 1D morphologies, including nanofibers, nanotubes, and core/shell structures.[35,36] Because no binders or conductive additives are used, the electrospun fiber papers have demonstrated high overall electrode capacities for Li-ion batteries.[38] Meanwhile, electrospray was also used to synthesize Si/C clusters with high capacity.[39] However, the Si/C particles have to be mixed with binders and carbon black and coated onto Cu current collectors, which lows the overall electrode capacity. If the electrospining and electrospray techniques are combined to in situ incorporate Si/C clusters into a carbon textile matrix (a 3D current collector) thus forming a nano-Si/carbon fiber paper, a binder-free and flexible Si/C paper electrode with high overall capacity, long cycle life, and high rate performance can be fabricated. The advantage of the combined electrospining/electrospray technology has been demonstrated by fabricating robust nanoparticle-on-nanofiber separators for Li-ion batteries.[40]

Here, 3D Si/C fiber paper anodes are, for the first time, fabricated by simultaneously electrospraying a nano-Si-polyacrylonitrile (PAN) dispersion and electrospinning a PAN solution to uniformly distribute PAN-coated nano-Si clusters into a PAN nanofiber paper (**Figure 1**), followed by carbonization in argon gas. The superior electrochemical performance of the novel 3D paper anodes is evident from the high overall capacity of 1600 mAh g^{-1} and high capacity retention of 840 mAh g^{-1} after 600 cycles. The excellent electrochemical performance and good flexibility make the 3D Si/C fiber paper anodes extremely attractive for paper batteries and wearable electronic clothing. In addition, this technology is facile, scalable, cost-effective, and suitable for mass production of paper batteries.

2. Results and Discussion

The synthesis procedure of the 3D Si/carbon fiber paper is schematically illustrated in Figure 1a. PAN was dissolved in dimethylformamide (DMF) to form a 6 wt% solution as the carbon fiber precursor. Si nanoparticles (diameter < 100 nm) were

dispersed in DMF using an ultrasonic process, and then PAN was added into the dispersion and stirred overnight. The PAN solution and Si/PAN dispersion were loaded into two syringes, which were driven by individual pumps. The concentrations of PAN in both PAN solution and Si-PAN dispersion were optimized to produce a fine fiber morphology and carbon-coated Si clusters with desired Si/C composition. The Si-to-C ratio can also be tuned by changing the electronspinning/spray speeds and the needle-to-collector distances. Composite paper with different total C-Si loading mass was prepared by changing the electrospinning/spray time. The polymer-based fiber/cluster paper (Figure 1b) was first stabilized at 250 °C in air, and then carbonized at 700 °C in Ar to form the final product of Si/C 3D paper (Figure 1c). Additional details are provided in the Experimental Section.

The as-synthesized Si/PAN paper is yellow-brown in color and highly flexible (**Figure 2**a). After carbonization, the Si/C composite film still maintained good flexibility, as shown in Figure 2b. The structure of the 3D Si/C fiber paper was investigated by scanning electron microscopy (SEM) (Figure 2c–f). The top view image in Figure 2c confirms that Si/C clusters were uniformly distributed among the carbon fabric to form the homogenous structure. Closer views (Figure 2d,e) clearly reveal that the electrospun carbon fibers with diameter of ≈200 nm formed a continuous carbon frame and microscale void space among the carbon fibers, which provide a fast electronic and ionic pathway, thus enhancing the reaction kinetics. Meanwhile, Si nanoparticles were bonded together by the coated carbon to form Si/C clusters with a diameter of 1–2 μm (Figure 2d). The clusters were also tightly wrapped into carbon fiber cages and embedded within the carbon fiber network. Since both carbons in the Si/C clusters and in the fiber matrix came from the same PAN, this results in strong bonding among the Si nanoparticles, Si/C clusters, and carbon fibers. The unoccupied fiber cages provide free space to accommodate the volume expansion of nano-Si. Therefore, the electrospun/sprayed 3D Si/C fiber structure can effectively alleviate stress/strain induced by the volume change, thus achieving long cycle life. The cross sectional image in Figure 2f shows the same architecture as the top view images, revealing the homogeneousness of the 3D structure through the entire Si/C fiber paper.

The structure nature of PAN-derived carbon was characterized using Raman spectroscopy, as shown in Supporting Information Figure S1. Two peaks at 1350 and 1600 cm^{-1} for the PAN carbon, corresponding to disordered (D) and graphitic (G) modes of carbon, respectively, are observed. The Raman spectrum reveals that carbon derived from PAN at 700 °C for 3 h in Ar gas is partially graphitic. The electric conductivity of the 3D Si/C fiber paper was measured to be 60 S cm^{-1} using the four probe method, which is more than two times higher than that of silicon nanoparticle–graphene paper composites that were prepared by reducing the self-assembled Si/Graphene oxides composites in the temperature range from 550 to 850 °C.[27]

Clearly, this novel structure of the 3D Si/C fiber composite paper offers many advantages as an anode for lithium ion batteries. First, the self-support structure avoids the use of binders, conductive additives, and heavy metal current collectors, which significantly increase the overall capacity. Second, the carbon fibers provide a conductive network, ensuring a good electric conductivity. Third, the large void space allows for accomodation of the large volume change during lithiation/delithiation and enables the electrolyte to sufficiently contact the Si particles to achieve fast kinetics. Fourth, the flexibility of the carbon fiber frame and carbon coating of the Si nanoparticles provide a mechanical support to avoid cracking of the electrode, thus maintaining electrode integrity. Finally, the same polymer precursor for carbon fibers and Si/C clusters was used, enabling a good connection over the entire carbon frame and Si particles. Good electrochemical performance is anticipated because of these features.

The composition of the 3D Si/C fiber composite paper was determined by thermogravimetric analysis (TGA) to be 72 wt% Si (Supporting Information Figure S2). Three electrodes with different total C-Si mass loadings of 0.8 mg cm^{-2}, 1.3 mg cm^{-2}, and 1.7 mg cm^{-2} were prepared, corresponding to Si loadings of 0.58 mg cm^{-2}, 0.94 mg cm^{-2}, and 1.22 mg cm^{-2}, respectively. The thickness of the 1.7 mg cm^{-2} sample was measured to be 30 μm, corresponding to a density of 0.567 g cm^{-3}. The loading

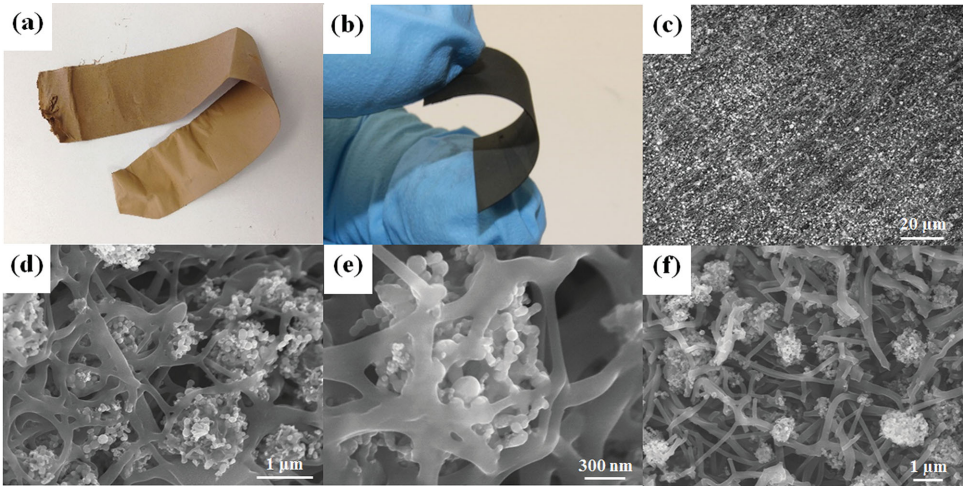

Figure 2. Photographs of the electrospun/sprayed flexible paper electrode a) before and b) after carbonization with 72 wt% Si. SEM images of the 3D Si/C fiber paper electrode: c–e) top view and f) cross section.

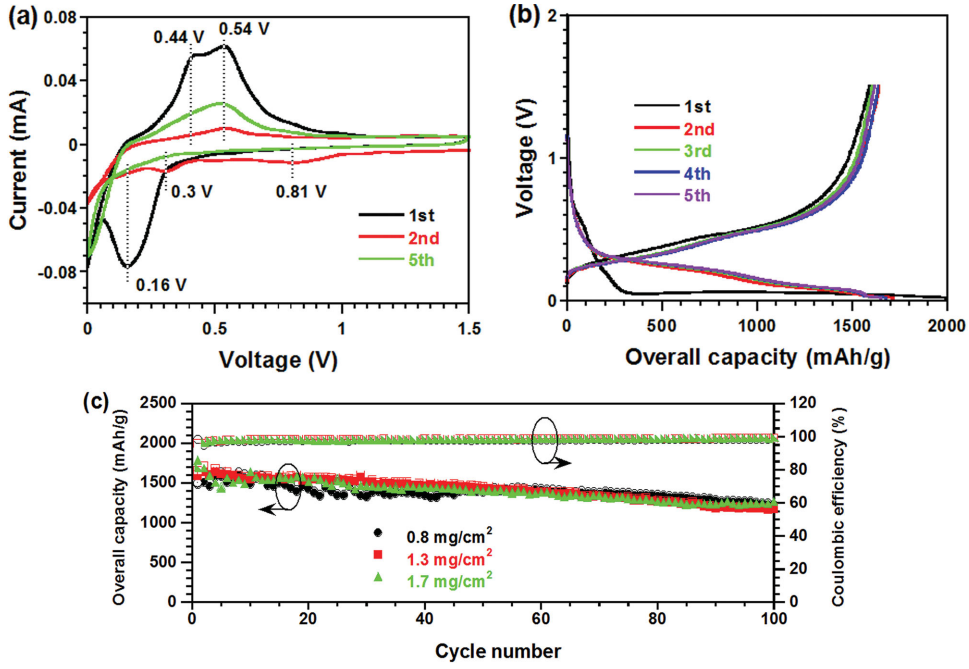

Figure 3. Electrochemical performance: a) CV curves of 1st, 2nd, and 5th cycles and b) charge/discharge profiles in the first five cycles of the flexible 3D Si/C fiber paper electrode. c) Cycling stability and Coulombic efficiency of the flexible 3D Si/C fiber paper electrodes with different overall loading mass of 0.8 mg cm^{-2}, 1.3 mg cm^{-2}, and 1.7 mg cm^{-2}.

mass is much higher than the traditional Si anodes prepared using slurry-coating method,[5–25] and also higher than those recent reported graphene or carbon nanotube-based Si paper anodes (Supporting Information Table S1).[1,2,27–34]

The electrochemical performance of the 3D Si/C fiber paper was evaluated in coin cells using the composite paper as anodes and lithium as counter electrodes. **Figure 3**a shows the cyclic voltammogram (CV) curves of the Si/C fiber paper anodes in the first, second, and fifth cycles. A broad cathodic peak centered at 0.81 V and a small cathodic peak at 0.3 V are observed in the first cycle but disappeared in the subsequent cycles; this is mainly attributed to the decomposition of the electrolyte to form solid-electrolyte interface (SEI) film. Strong cathodic peaks at 0.16 V and the cut-off voltage of 0 V correspond to the lithiation reaction of Si to form Li_xSi alloy. While the anodic peaks at 0.44 V and 0.54 V are assigned to the delithiation process of amorphous Li_xSi. The redox peaks are consistent with previous reports.[6]

Figure 3b shows the charge/discharge profiles of the 3D Si/C paper anodes with mass loading of 1.3 mg cm^2 in the first five cycles in a voltage window of 0.02–1.5 V with a current density of 500 mA g^{-1}. The first cycle shows a short slope plateau at a voltage of 0.8 V followed by a long flat plateau at 0.07 V. The slope plateau at 0.8 V is attributed to the decomposition of the electrolyte to form a SEI film, while the flat plateau at 0.07 V is characteristic of lithiation of crystalline Si. In the subsequent cycles, the crystal Si changed to amorphous Si and displayed typical charge/discharge profiles of amorphous Si. The first cycle delivered a delithiation capacity of 1996 mAh g^{-1} and a reversible capacity of 1589 mAh g^{-1}, corresponding to a Coulombic efficiency of 80%. Note that the capacities in this study were calculated based on the total weight of the 3D Si/C fiber paper. To the best of our knowledge, this is the highest capacity and Coulombic efficiency in the first cycle for carbon paper-based Si anodes.[27–34] Afterward, the Coulombic efficiency quickly jumped to higher than 98%, indicating a good reversibility.

Cycling stability of the three 3D Si/C paper anodes were tested at a current density of 500 mA g^{-1} and in the voltage window of 0.02–1.5 V (Figure 3c). Unlike previous reports on Si paper electrodes made from graphene sheets, where the increase in loading mass would significantly reduce the capacity and kinetics,[27] all three Si/C fiber paper electrodes with different Si loadings show stable cycling behavior, demonstrating the robustness of the 3D Si/C paper architecture. Moreover, all three anodes, regardless of the loading mass, also exhibit a similar stable capacity of about 1600 mAh g^{-1}, which is one order of magnitude higher than commercial graphite anodes[2] and much higher than all of the traditional Si anodes if the entire electrode mass is counted. In addition to high capacity, the 3D Si/C fiber paper electrodes were also proven to possess high cycling stability. After 100 cycles, very similar capacity retention of 1178–1267 mA g^{-1} was retained for the three anodes with different loading mass, which is much better than the carbon-paper Si anodes reported previously.[27–34]

The cumulative irreversible capacity of the 3D Si/C paper anodes with mass loading of 1.3 mg cm^2 in the first 100 cycles is shown in Supporting Information Figure S3. The cumulative irreversible capacity is critical for the commercialization of Si anodes due to the limitation of Li sources in the cathode. Although the Coulombic efficiency of the 3D Si/C paper anodes in the first two cycles jumped from 80% to 98% and the average Coulombic efficiency was higher than 99.8% after 100 cycles, which is comparable to or better than state-of-art Si/C paper

anodes reported in the literature,[28–34] cumulative irreversible capacity still continually increases with charge/discharge cycles at a gradually reduced rate and reached 2500 mAh g^{-1} at 100 cycles. The initial capacity (≈1600 mAh g^{-1}) would be lost after only 40 cycles based on the cumulative irreversible capacity (Supporting Information Figure S3). Although pre-lithiation can compensate for the initial irreversible capacity loss in the first cycle (≈400 mAh g^{-1}), the cumulative irreversible capacity still limits the cycling life of the Si anodes. Therefore, stabilization of Si SEI to reduce the cumulative irreversible capacity is essential for the commercialization of Si anodes in Li-ion batteries.

The electrochemical performance of the 3D Si/C fiber paper electrodes and all reported carbon paper Si anodes are compared in Supporting Information Table S1. Our 3D Si/C paper electrode shows the highest capacity and best cycling stability of Si/C fiber paper electrodes reported to date. The high overall capacity and long cycling stability, even at high Si loading, confirms the robustness of the 3D architecture of the Si/C paper prepared by electrospinning/spay, which can alleviate the stress/strain induced by lithium ion insertion/extraction and maintain a high activity of the entire 3D Si/C fiber structure.

Volumetric capacity of the 3D Si/C finber paper anodes with 1.7 mg cm^{-2} is shown in Supporting Information Figure S4. The volumetric capacity in the initial cycle is ≈1000 mAh cm^{-3}, which is more than two times higher than commercial graphite anodes (416 mAh cm^{-3})[46] and comparable to other free-standing film/paper Si electrodes.[46–48]

For comparison, electrosprayed nano-Si/C composites and PAN-derived carbon fiber paper were prepared under the same conditions as those used for the Si/C fiber paper. The cycling performance is shown in Supporting Information Figure S5. The electrodes of the electrosprayed nano-Si/C composites were prepared by casting slury containing 80 wt% composite: 10 wt% carbon black:10 wt% binder (Na-alginate). A higher initial reversible capacity was obtained but with a faster capacity fading with less than 50% capacity retention of the initial one for the cast electrosprayed anodes (Supporting Information Figure S5a), which is much lower than the 3D Si/C fiber paper anodes (75%) in this work. This demonstrates the superiority of the 3D Si/C fiber paper compared to the traditional casting Si anodes. The carbon fiber paper delievered a stable capacity of about 270 mAh g^{-1} but with a low initial Coulombic efficiency of 49.4% due to the formation of a large amount of SEI films on the surface of the carbon fibers (Supporting Information Figure S5b).

Extended cycling stability of the highest mass loading anodes (1.7 mg cm^{-2}) is shown in Supporting Information Figure S6. After 600 cycles, it retained a capacity of 840 mAh g^{-1}, which is more than four times higher than that of graphite anodes and one order of magnitude higher than those of traditional Si anodes. As shown in Supporting Information Table S1, most of the Si/C paper electrode can only survive 100 cycles or fewer, with much lower capacity retention. For example, in recent work, Ji et al. used graphite foam as the current collector for Si, but it showed a low initial capacity of 983 mAh g^{-1} and quick capacity loss to 370 mAh g^{-1} after 100 cycles,[2] i.e., much lower than the 600-cycle capacity retention in this work.

The robustness of electrospun/sprayed 3D Si/C fiber paper electrode with 1.7 mg cm^{-2} loading was also evident from the similarity of the morphology and architecture before and after 100 full charge/discharge cycles (**Figure 4**). Figure 4a shows the photograph after 100 cycles. In comparison with the fresh samples (Figure 2b), no cracks or fragments of the Si/C fiber paper anodes were observed. The microstructure of the 3D Si/C fiber paper after 100 cycles is shown in the SEM images in Figure 4b. Due to volume expansion of nano-Si and the formation of SEI, the porosity of the 3D Si/C fiber paper was significantly reduced compared to the fresh 3D Si/C fiber paper in Figure 2. However, the Si/C clusters were still tightly embedded within the carbon fiber networks after 100 cycles, and the carbon fibers have an intimate connection in the paper electrode, maintaining the integrity of the 3D Si/C fiber paper electrodes.

The 3D Si/C fiber paper anodes also show excellent rate capability. **Figure 5**a shows the capacity retention of the 3D Si/C fiber paper electrodes with a mass loading of 1.7 mg cm^{-2} as the current density increased from 0.2 A g^{-1} to 8 A g^{-1}. Even at much a high current density of 8 A g^{-1}, the overall capacity still retained ≈500 mAh g^{-1}, which is much higher than all other Si/C paper anodes reported in literature (Supporting Information Table S1). Figure 4b shows the charge/discharge curves at different current rates. The 3D Si/C fiber paper electrodes clearly show the lithiation/delithiation plateaus of Si, even at high rates, which benefit from the fast kinetics and good conductivity of the 3D paper electrodes.

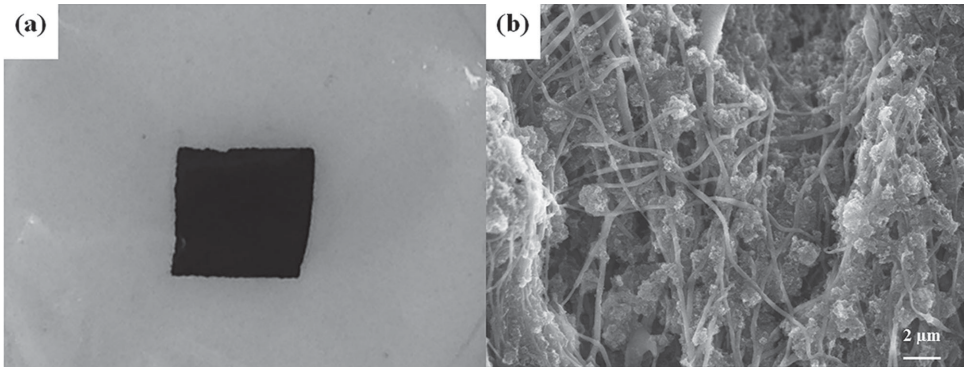

Figure 4. a) Photograph and b) SEM image of the flexible 3D Si/C fiber paper electrode after 100 cycles.

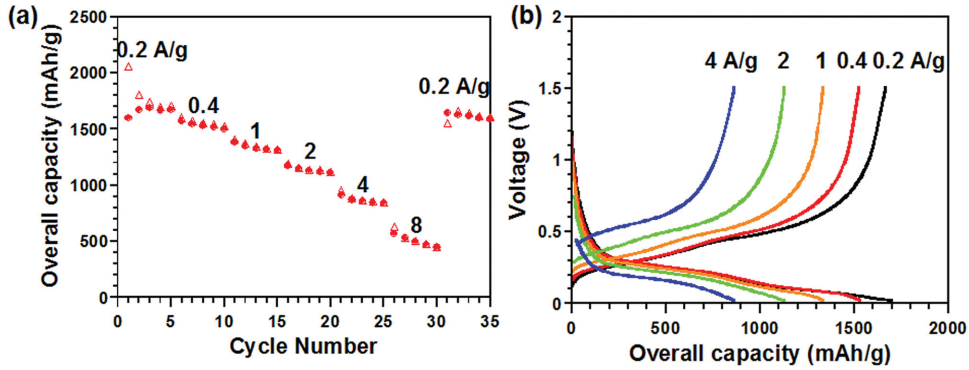

Figure 5. Rate capability of the flexible 3D Si/C fiber paper electrode. a) Capacity retention and b) voltage profiles at current density from 0.2 A g^{-1} to 4 A g^{-1}.

3. Conclusion

We report a novel flexible 3D Si/C fiber paper electrodes with high Si loading of 1.2 mg cm^{-2} for lithium ion batteries. The overall electrode capacity of ≈1600 mAh g^{-1} is one order of magnitude higher than commercial graphite anodes and also much higher than all other Si paper anodes reported to date. The flexible 3D Si/C fiber paper electrode still retained a capacity of as high as 840 mAh g^{-1} after extended cycling stability tests of 600 cycles, which is considerably higher than other carbon-paper-based Si anodes. Most importantly, the electrochemical performance of the flexible 3D Si/C fiber paper electrode is not sensitive to the loading mass, thus revealing a robustness of our 3D Si/C paper electrodes. The superior electrochemical performance of the flexible Si/C 3D paper electrodes is believed to be associated with the unique architecture: resiliency and conductivity of the carbon fiber network, porosity of the matrix, carbon-coating of the Si nanoparticles, strong adhesion between the carbon fibers and Si/C clusters, and uniform distribution of the Si/C clusters in the carbon fiber frame. In addition to the electrochemical performance, the combined electrospinning/electrospray technology is suitable for mass production with a low cost. This new fabrication strategy can be used to prepare battery electrodes and can be extended to other flexible composite materials for broader flexible electronics.

4. Experimental Section

Synthesis of the 3D Si/C Fiber Paper: The synthesis was an in situ process incorporating Si/polymer clusters produced by electrospray into the electrospun fibers. PAN was dissolved in DMF to form a 6 wt% solution as the carbon fiber precursor for electrospinning. Meanwhile, 0.16 g crystalline Si nanoparticles (diameter <100 nm) were dispersed in 4 mL DMF by ultrasonic treatment for 30 min, and then 0.12 g PAN was added to the dispersion followed by vigorous stirring overnight as Si/C cluster source. The PAN solution and Si/PAN dispersion were loaded into two syringes, which were driven by individual pumps. Needles with 27-gauge and 23-gauge sizes were used for electrospinning and electrospray, respectively. A grounded roller was used as a product collector. The collector-to-needle distance was 15 cm and 10 cm for the electrospinning and electrospray, respectively. The same working voltage of 17 kV was applied for both of electrospinning and electrospray. The electrospinning speed was 0.4 mL h^{-1}, while the speed for electrospray was 0.5 mL h^{-1}. The voltage, collector-to-needle distance, and speed could be independently varied to optimize the fiber quality and 3D architecture. The resulting composite paper was first stabilized at 250 °C in air for 3 h with a ramp rate of 1 °C min^{-1}. It then underwent heat treatment at 700 °C for 3 h in Ar gas with a heating rate of 5 °C min^{-1} to produce the final Si/C fiber paper. The thicknesses for the paper electrodes with 0.8, 1.3, and 1.7 mg cm^{-2} loadings were 14, 23, 30 μm, respectively.

Material Characterizations: SEM images were acquired with a Hitachi SU-70 analytical ultra-high resolution SEM (Japan). Thermogravimetric analysis (TGA) was carried out using a thermogravimetric analyzer (TA Instruments, USA) with a heating rate of 10 °C min^{-1} in air. Raman measurements were performed on a Horiba Jobin Yvon Labram Aramis using a 532 nm diode-pumped solid-state laser.

Electrochemical Measurements: The final flexible 3D Si/C fiber paper was cut into pieces with size 5 mm × 5 mm and directly used as anodes. Electrochemical performance was tested in CR2032 coin cells, which were assembled with lithium foil as the counter electrode, 1 M $LiPF_6$ in a mixture of fluoroethylene carbonate/dimethyl carbonate (FEC/DMC, 1:1 by volume) as the electrolyte, and Celgard3501 (Celgard, LLC Corp., USA) as the separator. Electrochemical performance was tested using an Arbin battery test station (BT2000, Arbin Instruments, USA) at voltage of 0.02–1.5 V with different current densities. Capacity was calculated on the basis of total mass of the entire Si/C fiber paper. CV data were collected using a Solatron 1260/1287 Electrochemical Interface (Solartron Metrology, UK). For comparison, electrosprayed nano-Si/C composites and PAN-derived carbon fiber papers were prepared under the same conditions as those used for the Si/C fiber paper. The electrochemical performance of the nano-Si/C electrodes with a weight ratio of 8:1:1 of Si/C composite:carbon black:binder (Na-alginate) prepared by casting Si/C onto copper foil was tested.

Supporting Information

Supporting Information is available from the Wiley Online Library or from the author.

Acknowledgements

The authors gratefully acknowledge the support of the Army Research Office under Contract No.: W911NF1110231.

Received: May 6, 2014
Revised: July 24, 2014
Published online:

[1] K. Evanoff, J. Benson, M. Schauer, I. Koyalenko, D. Lashmore, W. J. Ready, G. Yushin, *ACS Nano* **2012**, *6*, 9837.
[2] J. Ji, H. Ji, L. L. Zhang, X. Zhao, X. Bai, X. Fan, F. Zhang, R. S. Ruoff, *Adv. Mater.* **2013**, *25*, 4673.
[3] U. Kasavajjula, C. S. Wang, A. J. Appleby, *J. Power Sources* **2007**, *163*, 1003.
[4] H. Wu, Y. Cui, *Nano Today* **2012**, *7*, 414.
[5] I. Kovalenko, B. Zdyrko, A. Magasinski, B. Hertzberg, Z. Milicev, R. Burtovyy, I. Luzinov, G. Yushin, *Science* **2011**, *334*, 75.
[6] Y. Wen, Y. J. Zhu, A. Langrock, A. Manivannan, S. H. Ehrman, C. S. Wang, *Small* **2013**, *9*, 2810.
[7] Y.-S. Hu, R. Demir-Cakan, M.-M. Titirici, J.-O. Müller, R. Schlögl, M. Antonietti, J. Maier, *Angew. Chem. Int. Ed.* **2008**, *47*, 1645.
[8] S. H. Ng, J. Wang, D. Wexler, K. Konstantinov, Z.-P. Guo, H.-K. Liu, *Angew. Chem. Int. Ed.* **2006**, *45*, 6896.
[9] A. Magasinski, P. Dixon, B. Hertzberg, A. Kvit, J. Ayala, G. Yushin, *Nat. Mater.* **2010**, *9*, 353.
[10] C. Chan, H. Peng, G. Liu, K. Mcilwrath, X. F. Zhang, R. A. Huggins, Y. Cui, *Nat. Nanotechnol.* **2008**, *3*, 31.
[11] L. F. Cui, R. Ruffo, C. K. Chan, H. L. Peng, Y. Cui, *Nano Lett.* **2009**, *9*, 491.
[12] H. Wu, G. Chan, J. W. Choi, I. Ryu, Y. Yao, M. T. Mcdowell, S. W. Lee, A. Jackson, Y. Yang, L. Hu, Y. Cui, *Nat. Nanotechnol.* **2012**, *7*, 310.
[13] M.-H. Park, M. G. Kim, J. Joo, K. Kim, J. Kim, A. Ahn, Y. Cui, J. Cho, *Nano Lett.* **2009**, *9*, 3844.
[14] T. H. Hwang, Y. M. Lee, B.-S. Kong, J.-S. Seo, J. W. Choi, *Nano Lett.* **2012**, *12*, 802.
[15] L. W. Ji, X. W. Zhang, *Electrochem. Commun.* **2009**, *11*, 1146.
[16] H. Kim, B. Han, J. Choo, J. Cho, *Angew. Chem. Int. Ed.* **2008**, *47*, 10151.
[17] D. S. Jung, T. H. Hwang, S. B. Park, J. W. Choi, *Nano Lett.* **2013**, *13*, 2092.
[18] R. Yi, F. Dai, M. L. Gordin, S. Chen, D. Wang, *Adv. Energy Mater.* **2013**, *3*, 295.
[19] Y. Yao, M. T. Mcdowell, I. Ryu, H. Wu, N. Liu, L. Hu, W. D. Nix, Y. Cui, *Nano Lett.* **2011**, *11*, 2949.
[20] H. Wu, G. Zheng, N. Liu, T. J. Carney, Y. Yang, Y. Cui, *Nano Lett.* **2012**, *12*, 904.
[21] A. Gohier, B. Laïk, K.-H. Kim, J.-L. Maurice, C. S. Pereira-Ramojocaru, P. T. Van, *Adv. Mater.* **2012**, *24*, 2592.
[22] W. Wang, P. N. Kumta, *ACS Nano* **2010**, *4*, 2233.
[23] X. Zhou, Y.-X. Yin, L.-J. Wan, Y.-G. Guo, *Adv. Energy Mater.* **2012**, *2*, 1086.
[24] B. Wang, X. Li, X. Zhang, B. Luo, Y. Zhang, L. Zhi, *Adv. Mater.* **2013**, *25*, 3560.
[25] J. Deng, H. Ji, C. Yan, J. Zhang, W. Si, S. Baunack, S. Oswald, Y. Mei, O. G. Schmidt, *Angew. Chem. Int. Ed.* **2013**, *52*, 2326.
[26] J. C. Guo, A. Sun, C. S. Wang, *Electrochem. Commun.* **2010**, *12*, 981.
[27] J. K. Lee, K. B. Smith, C. M. Hayner, H. H. Kung, *Chem. Commun.* **2010**, *46*, 2025.
[28] J.-Z. Wang, C. Zhong, S.-L. Chou, H.-K. Liu, *Electrochem. Commun.* **2010**, *12*, 1467.
[29] C. Pang, H. Cui, G. Yang, C. Wang, *Nano Lett.* **2013**, *13*, 4708.
[30] L. Hu, H. Wu, Y. Cao, A. Cao, H. Li, J. Mcdough, X. Xie, M. Zhou, Y. Cui, *Adv. Energy Mater.* **2011**, *1*, 523.
[31] C.-F. Sun, H. L. Zhu, E. B. Baker III, M. Okada, J. Wan, A. Ghemes, Y. Inoue, L. Hu, Y. Wang, *Nano Energy* **2013**, *2*, 987.
[32] Y. Fu, A. Manthiram, *Nano Energy* **2013**, *2*, 1107.
[33] S.-L. Chou, Y. Zhao, J.-Z. Wang, Z.-X. Chen, H.-K. Liu, S.-X. Dou, *J. Phys. Chem. C* **2010**, *114*, 15862.
[34] L. Yue, H. Zhong, L. Zhang, *Electrochim. Acta* **2012**, *76*, 326.
[35] D. Li, Y. N. Xia, *Adv. Mater.* **2004**, *16*, 1151.
[36] A. Greiner, J. H. Wendorff, *Angew. Chem. Int. Ed.* **2007**, *46*, 5670.
[37] X. Zhou, L.-J. Wan, Y.-G. Guo, *Small* **2013**, *9*, 2684.
[38] Y. Zhu, X. Han, Y. Xu, Y. Liu, S. Zheng, K. Xu, L. Hu, C. Wang, *ACS Nano* **2013**, *7*, 6378.
[39] Y.-X. Yin, S. Xin, L.-J. Wan, C.-J. Li, Y.-G. Guo, *J. Phys. Chem. C* **2011**, *115*, 14148.
[40] M. Yanilmaz, L. Yao, M. Dirican, K. Fu, X. Zhang, *J. Membr. Sci.* **2014**, *456*, 57.
[41] L. Ji, Z. Lin, M. Alcoutlabi, X. Zhang, *Energy Environ. Sci.* **2011**, *4*, 2682.
[42] L. Ji, X. Zhang, *Carbon* **2009**, *47*, 3219.
[43] L. Ji, X. Zhang, *Energy Environ. Sci.* **2010**, *3*, 124.
[44] L. Ji, K. Jung, A. J. Medford, X. Zhang, *J. Mater. Chem.* **2009**, *19*, 4992.
[45] Y. Li, B. Guo, L. Ji, Z. Lin, G. Xu, Y. Liang, S. Zhang, O. Toprakci, Y. Hu, M. Alcoutlabi, X. Zhang, *Carbon* **2013**, *51*, 185.
[46] S. Jeong, J.-P. Lee, M. Ko, G. Kim, S. Park, J. Cho, *Nano Lett.* **2013**, *13*, 3403.
[47] J. W. Choi, L. B. Hu, L. F. Cui, J. R. Mcdonough, Y. Cui, *J. Power Sources* **2010**, *195*, 8311.
[48] A. M. Chockla, J. T. Harris, V. A. Akhavan, T. D. Bogart, V. C. Holmberg, C. Steinhagen, C. B. Mullins, K. J. Stevenson, B. A. Korgel, *J. Am. Chem. Soc.* **2011**, *133*, 20914.